doi: 10.18323/2782-4039-2024-4-70-5

On the formation of thermal barrier coatings by magnetron sputtering

Gennady V. Kachalin[1], PhD (Engineering), leading researcher
Konstantin S. Medvedev[2], leading engineer
Aleksey F. Mednikov[3], PhD (Engineering), leading researcher
Olga S. Zilova[4], PhD (Engineering), leading researcher
Aleksandr B. Tkhabisimov*[5], PhD (Engineering), senior researcher
Dmitriy I. Ilyukhin[6], engineer of the 1st category
Vladislav A. Kasyanenko[7], engineer of the 1st category
National Research University "Moscow Power Engineering Institute", Moscow (Russia)

***E-mail:** TkhabisimovAB@mpei.ru, abt-bkt@mail.ru

[1]ORCID: https://orcid.org/0000-0001-9506-862X
[2]ORCID: https://orcid.org/0000-0003-1667-458X
[3]ORCID: https://orcid.org/0000-0003-4883-7873
[4]ORCID: https://orcid.org/0000-0002-0410-8188
[5]ORCID: https://orcid.org/0000-0001-9544-9086
[6]ORCID: https://orcid.org/0009-0009-6385-0284
[7]ORCID: https://orcid.org/0009-0000-7510-2106

Received 18.10.2024 *Revised 26.11.2024* *Accepted 03.12.2024*

Abstract: The use of magnetron sputtering systems with extended uncooled targets will allow developing industrial import-substituting technologies for the formation of thermal barrier coatings, based on zirconium oxide doped with rare earth metal oxides to solve urgent problems of gas turbine construction. This paper presents the results of comparing the technology for producing thermal barrier coatings by magnetron sputtering, with two types of extended targets made of Zr–8%Y alloy – a widely used cooled target and an uncooled extended target, of a magnetron sputtering system developed by the authors. This paper gives a comparison of the results of mass-spectrometric studies of the hysteresis of the oxygen partial pressure inherent in the technology for producing oxide films; the influence of the target type on the coating growth rate; studies of the structure of thermal barrier coatings using the scanning electron microscopy method; and the elemental composition of coatings based on zirconium dioxide partially stabilised with yttrium oxide – YSZ. It has been experimentally found that increasing the temperature of the magnetron sputtering system target, allows decreasing the loop width of the characteristic hysteresis of the oxygen partial pressure dependence on its flow rate by 2 times. The obtained dependencies allowed determining the range of oxygen flow rates at various magnetron discharge powers, at which the work can be performed with stable and sustainable process control, without the risk of falling into hysteresis. The conducted metallographic studies showed a characteristic developed porous dendritic structure of the ceramic layer, which is necessary to reduce the thermal conductivity coefficient of the thermal barrier coating. It has been revealed that the use of an uncooled target allows increasing the deposition rate of the thermal barrier coating by more than 10 times compared to the deposition rate for a cooled target. The obtained results demonstrate the possibility of using the magnetron sputtering technology of an extended uncooled target to form a ceramic layer of thermal barrier coatings.

Keywords: magnetron sputtering; uncooled target; thermal barrier coatings; hysteresis phenomena; coating deposition rate.

Acknowledgements: State assignment No. FSWF-2023-0016 (Agreement No. 075-03-2023-383 dated January 18, 2023) in the field of scientific activity for 2023–2025.

For citation: Kachalin G.V., Medvedev K.S., Mednikov A.F., Zilova O.S., Tkhabisimov A.B., Ilyukhin D.I., Kasyanenko V.A. On the formation of thermal barrier coatings by magnetron sputtering. *Frontier Materials & Technologies*, 2024, no. 4, pp. 51–61. DOI: 10.18323/2782-4039-2024-4-70-5.

INTRODUCTION

The problems of ensuring the reliability of aircraft gas turbine engines (GTE) and power gas turbine plants (GTP) are the most complex among the numerous problems arising in the development of modern gas turbines. The most important element of a gas turbine is the rotor blades, the material and design of which largely determine the service life and permissible temperature of the gas in front of the turbine.

The temperatures of combustion products in gas turbines reach 1700 °C, therefore, thermal barrier coatings (TBC) are used to protect the rotor blades from high-temperature exposure.

Modern thermal barrier coatings are heat-resistant composite coatings with a thickness of 100÷400 μm consisting of two layers. The first (lower) layer is a metal heat-resistant binder, usually of the *Me*CrAlY type, where *Me* is the γNi or Co matrix, which protects the substrate material from oxidation and creates an adhesive pair with the second (upper) layer, – a ceramic heat-insulating coating consisting of rare earth metal oxides and having low thermal conductivity [1; 2]. The first TBC layer protects the substrate material from oxidation (the coefficient of heat expansion of the layer can reach $16.8 \cdot 10^{-6}$ K^{-1} from room temperature to 1000 °C) [3; 4]. The second layer is a heat-insulating layer with low thermal conductivity (about 0.8÷1.2 W/(m·K)) and high resistance to thermal cycling [5].

Among the wide range of ceramic materials, the most interesting one as the upper ceramic coating layer is zirconium dioxide with additives of rare earth metal oxides, in particular stabilised with yttrium oxide – 8%Y_2O_3 (yttria-stabilised zirconia, YSZ). This ceramic composition has low thermal conductivity, high strength, fracture toughness, wear resistance and heat expansion coefficient comparable with the metal first layer of TBC [6]. The use of YSZ is necessary to stabilise pure ZrO_2, since its monoclinic structure transforms into tetragonal and cubic phases, when exposed to high temperature leading to the development of stresses [7; 8]. It is noted that the monoclinic-tetragonal transition in ZrO_2 occurs with a destructive change in volume, which hinders the manufacture and use of products made of pure oxide [9].

The most widely used methods for forming TBCs are electron beam evaporation and plasma deposition in air and vacuum. Formation of coatings in vacuum allows depositing films with high adhesion to the substrate, but requires a large consumption of target material with a low utilisation factor (0.15–0.25) [8]. In turn, the application of electron beam evaporation and plasma deposition in air allows forming coatings with a high deposition rate and high resistance to thermal cycling, but it is often difficult due to the limited availability of materials, and the impossibility of coating parts with complex shapes [10; 11].

At the same time, one can argue that, due to the development of magnetron sputtering technologies, this method can become an alternative to existing ones. This is caused by the fact that when temperatures rise above 1300 °C, the standard YSZ material approaches certain limitations due to sintering, and phase transformations at elevated temperatures. YSZ formed during electron beam evaporation and plasma deposition in air consists of a metastable t'-phase. When exposed to elevated temperatures for a long time, it decomposes into phases with high and low yttrium content. The latter, upon cooling, transforms into a monoclinic phase with a corresponding significant increase in volume, which ultimately leads to the destruction of the coating [12–14].

The main difficulty in implementing standard magnetron sputtering, with a cooled target to obtain TBCs, is the formation of a thin non-conducting film of an oxide compound on its surface during the occurrence of reactive processes in the presence of oxygen. Such oxide films have high electrical resistance, which prevents the flow of sputtering ion currents [15].

The work [16] presents the results of the study of the temperature dependence of the specific resistance of ZrO_2-based ceramics, which showed that in the temperature range from 500 to 1000 K, the specific resistance decreases, and the conductivity of the thin oxide film at a temperature above 1000 K is sufficient for stable combustion of the magnetron discharge. Under the influence of heating from ion bombardment, the specific resistance of the YSZ oxide formed on the surface of the uncooled target decreases, and it can be sputtered.

Fig. 1 shows the dependence of the growth rate of the ZrYO coating obtained by sputtering a zirconium target on the oxygen consumption. At an oxygen consumption of more than 3.0 units, the growth rate of the coating drops sharply due to the target surface oxidation. In the oxygen consumption range of 0–3.0 units, a "metallic mode" is realised, in which the deposition rate is about 4 μm/h, and opaque metallic-colored coatings conducting electric current are formed. Such coatings cannot be used as TBC, since when heated in an air environment they burn and peel off.

At oxygen consumption of more than 4.0 units, the "oxidised mode" is realised and transparent and non-conductive coatings are formed, which can be used as TBC, however, the deposition rate of such coatings decreases sharply and is about 0.3 μm/h (Fig. 1). To apply a ceramic TBC layer 50 μm thick under the conditions of the experiments, it would take more than 160 h, which is ineffective for industrial application of ceramic TBC layers, using magnetron sputtering systems with a cooled target.

The solution to the problem of TBC formation by magnetron sputtering can be the use of uncooled targets, heated to a temperature of more than 1000 °C. At these temperatures, oxide films formed on the surface of an uncooled target have electrical conductivity, and do not hinder the magnetron discharge combustion. Due to the high temperature, it is possible as well to evaporate the uncooled target material, which creates an additional flow of atoms from the surface, and allows increasing the deposition rate of the coating [17–19].

The main functional property of the thermal barrier coating is the thermal conductivity coefficient; for YSZ coatings, it is the lowest among oxide systems. A further decrease in the thermal conductivity coefficient is achieved by growth methods – conditions are created for the growth of a porous structure in the form of feathers (dendrites) [20].

The presented analysis showed that a logical stage in the development of the magnetron sputtering technology, with a cooled target for producing TBC with a minimum thermal conductivity coefficient, is the transition to the use of a magnetron sputtering system with an uncooled target. This causes the necessity of comparing two types of targets, based on the results of experimental studies of the hysteresis of the oxygen partial pressure, inherent in the technology of producing oxide films; the effect of the target type on the growth rate of the coating; determination of the structure, and elemental composition of YSZ thermal barrier coatings obtained using an uncooled target.

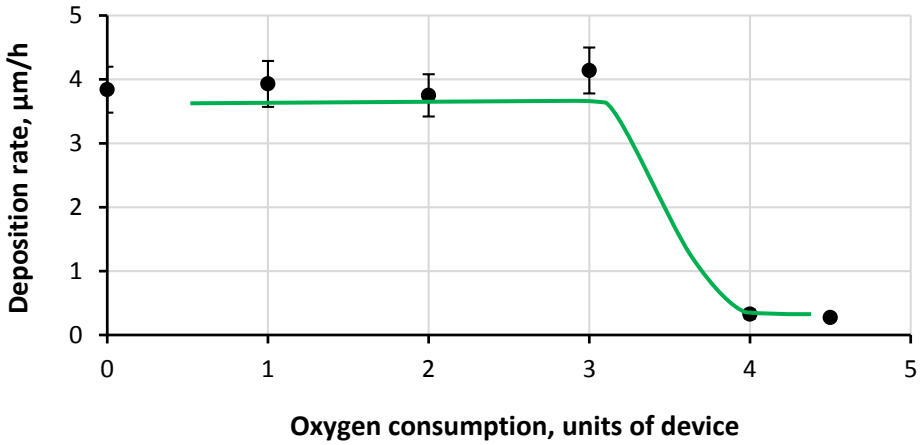

Fig. 1. *Dependence of the deposition rate of the ZrYO-based coating on oxygen consumption at a magnetron discharge power of 5 kW (cooled target).*
Source: Kachalin G.V., Mednikov A.F., Medvedev K.S., Bychkov A.I., Zilova O.S. Study of the influence of oxygen consumption on the deposition rate of Zr–Y-based coatings at magnetron sputtering with a cooled target. Vakuumnaya tekhnika i tekhnologii – 2023: sbornik trudov 30-y Vserossiyskoy nauchno-tekhnicheskoy konferentsii s mezhdunarodnym uchastiem. Sankt-Petersburg, Sankt-Peterburgskiy gosudarstvennyy elektrotekhnicheskiy universitet "LETI" im. V.I. Ulyanova (Lenina) Publ., 2023, pp. 108–113. EDN: GTVAVJ
Рис. 1. *Зависимость скорости осаждения покрытия на основе ZrYO от расхода кислорода при мощности магнетронного разряда 5 кВт (охлаждаемая мишень).*
Источник: Качалин Г.В., Медников А.Ф., Медведев К.С., Бычков А.И., Зилова О.С. Изучение влияния расхода кислорода на скорость осаждения покрытия на основе Zr–Y при магнетронном распылении с охлаждаемой мишенью // Вакуумная техника и технологии – 2023: сборник трудов 30-й Всероссийской научно-технической конференции с международным участием. СПб.: Санкт-Петербургский государственный электротехнический университет «ЛЭТИ» им. В.И. Ульянова (Ленина), 2023. С. 108–113. EDN: GTVAVJ

The aim of this study is to develop a technology for the formation of thermal barrier coatings, based on zirconium dioxide partially stabilised with yttrium oxide, using magnetron sputtering of an extended uncooled target.

METHODS

The coatings were formed using a vacuum unit developed at the National Research University "Moscow Power Engineering Institute". Fig. 2 shows the schematic diagram of the process unit working volume.

A special feature of the unit is the presence of a rotation system that provides the possibility of both planetary rotation of the processed products and samples and rotation of all or separately selected items of the planetary mechanism in a given position, in particular, directly in front of the magnetron sputter target.

The coatings were formed using a planar magnetron (developed by the National Research University "Moscow Power Engineering Institute", Russia) with an extended target measuring 710×80×8 mm, made of 92%Zr–8%Y alloy. During the process, stainless steel samples were fixed on equipment that rotated directly in front of the magnetron. The distance from the target to the rotation axis was 150 mm. Argon and oxygen of special purity supplied to the vacuum chamber using RRG-10 gas flow regulators were used as the process gases.

The technological process of coating formation, included pumping out the vacuum chamber to a pressure of $5 \cdot 10^{-3}$ Pa combined with heating the chamber and equipment, and supplying plasma-forming argon gas to perform ion cleaning of samples in a glow discharge in the area of magnetrons with cooled targets. Then the samples were moved to a preheated uncooled target (Fig. 3), and the coating was formed with continuous rotation of the samples in front of the target.

The magnetron discharge power varied in the range from 2.2 to 9 kW. For experiments with a cooled target, coatings were formed immediately after the ion cleaning stage.

The uncooled target temperature was measured by a chromel-alumel thermocouple placed in a channel, drilled in the side end of the target so that the thermocouple junction was located near the magnetron discharge track.

Studies of the surface microstructure and morphology, thickness and composition of the resulting coatings, elemental analysis were carried out using the control and measuring equipment, included in the experimental complex of the Unique Scientific Facilities (USF) "Erosion-M Hydraulic Impact Test Facility" of the National Research University "Moscow Power Engineering Institute".

The microstructure and morphology of the coating surface were studied using a TESCAN MIRA 3 LMU high-resolution scanning electron microscope (Tescan, Czech Republic) with a Schottky-electron emitter. Elemental analysis of the coatings was performed by energy-dispersive X-ray spectrometry, using an Oxford X Max 50 EDS spectrometer (Oxford Instruments, UK), mounted on a TESCAN MIRA 3 LMU microscope. The microstructure and composition of the coatings by depth were studied on transverse metallographic sections made using a Buehler GmbH sample preparation complex (Buehler, USA).

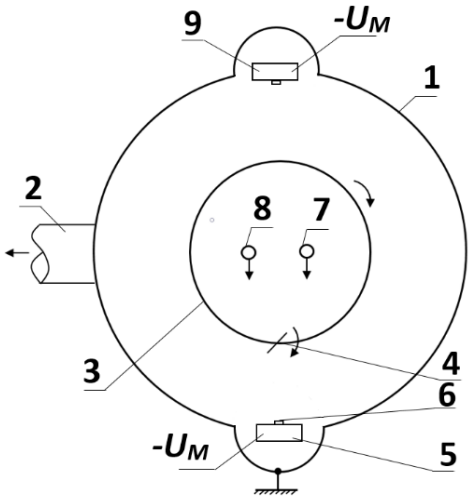

Fig. 2. *Scheme of the technological installation for applying thermal barrier coating with a magnetron with an extended uncooled target:*
1 – vacuum chamber; 2 – high vacuum pumping pipe; 3 – planetary carousel;
4 – sample; 5 – magnetron source; 6 – uncooled target;
7 – argon supply; 8 – oxygen supply;
9 – magnetron for ion purification of samples
Рис. 2. *Схема технологической установки нанесения термобарьерного покрытия магнетроном с протяженной неохлаждаемой мишенью:*
1 – вакуумная камера; 2 – патрубок высоковакуумной откачки;
3 – планетарная карусель; 4 – образец; 5 – магнетронный источник;
6 – неохлаждаемая мишень; 7 – подача аргона; 8 – подача кислорода;
9 – магнетрон ионной очистки образцов

a

b

Fig. 3. *The appearance of the uncooled Zr–Y target:*
a *– before the discharge is turned off;* ***b*** *– after the discharge is turned off*
Рис. 3. *Внешний вид неохлаждаемой мишени Zr–Y:*
a *– до выключения разряда;* ***b*** *– после выключения разряда*

The coating thickness was determined both on transverse sections during surface microstructure examination on a TESCAN MIRA 3 LMU microscope, and by ball grinding using a Calotest Compact device (Anton Paar, Austria). The deposition rate was calculated based on the results of determining the thickness and time of coating formation.

The composition of the atmosphere in the vacuum chamber was studied using a Pfeiffer Vacuum Prisma-Plus quadrupole mass spectrometer (Pfeiffer Vacuum,

Germany), equipped with differential pumping. The influence of the oxygen flow rate and magnetron discharge power on the partial pressure of argon and oxygen was studied, using the mass-spectrometric method of analysing the composition of the gas atmosphere in the vacuum chamber cap.

RESULTS

Fig. 4 shows a typical dependence of the partial pressure of oxygen on its flow rate for the formation of an YSZ coating by magnetron sputtering with cooled and uncooled targets.

It is evident that the dependences of the partial pressure of oxygen in the chamber on its flow rate are nonlinear with a pronounced hysteresis. At the same oxygen consumption, two values of partial pressure are observed depending on the direction of change in the oxygen consumption, and for a cooled target, the change in the partial pressure of oxygen is greater than for an uncooled target.

In the case of a cooled target, with an oxygen consumption above 2.5 units, a sharp increase in the partial pressure of oxygen was observed, which tended to saturate at a flow rate of more than 4.5 units (Fig. 4). This indicates a corresponding sharp decrease in the sputtering rate of the cooled target, due to the formation of an oxide film and a decrease in the number of sputtered zirconium and yttrium atoms that bind oxygen. With decreasing oxygen consumption, its partial pressure decreases, and with an oxygen consumption of 0.5 units, the target is completely cleared of the formed oxide film.

The derivatives of the direct and inverse dependencies of the partial pressure of oxygen on its consumption differ several times. Their type depends on the holding time at each value of oxygen consumption, as well as the stage of formation or etching of the oxide film on the target surface. It is noted that the controllability of the formation process on the inverse dependence is much more stable. The partial pressure of oxygen increases from 0 to 32 %, with an increase in oxygen consumption from 2.0 to 4.5 units, but decreases to 0 % with a decrease in oxygen consumption from 4.5 to 0.5 units.

In turn, for an uncooled target, the obtained dependencies are shifted to the region of higher oxygen consumption values (Fig. 4). The partial pressure begins to increase at an oxygen consumption of 3.5 units, which indicates a significantly higher sputtering rate of the uncooled target. Thus, at an oxygen consumption of 4.0 units on a cooled target, the partial pressure of oxygen in the chamber was 30 %, while on an uncooled target its value is close to zero, i.e. all the incoming oxygen is absorbed by the growing YSZ layer. The obtained dependencies for an uncooled target change monotonically, and the revealed maximum value of the partial pressure of oxygen is 1.5 times less than for a cooled target.

A feature of the reverse branch of the dependence for an uncooled target is the presence of a section with an oxygen consumption of 4.5–5.5 units, with an almost unchanged partial pressure and a derivative value close to zero (Fig. 4). From the point of view of the TBC formation technology, the presence of such a section indicates that work in this area can be performed with stable process control, without the risk of falling into hysteresis. Achieving process stability is possible with a smooth increase in oxygen consumption values from 0.0 to more than 7.0 units and a subsequent decrease to 4.5–5.5 units.

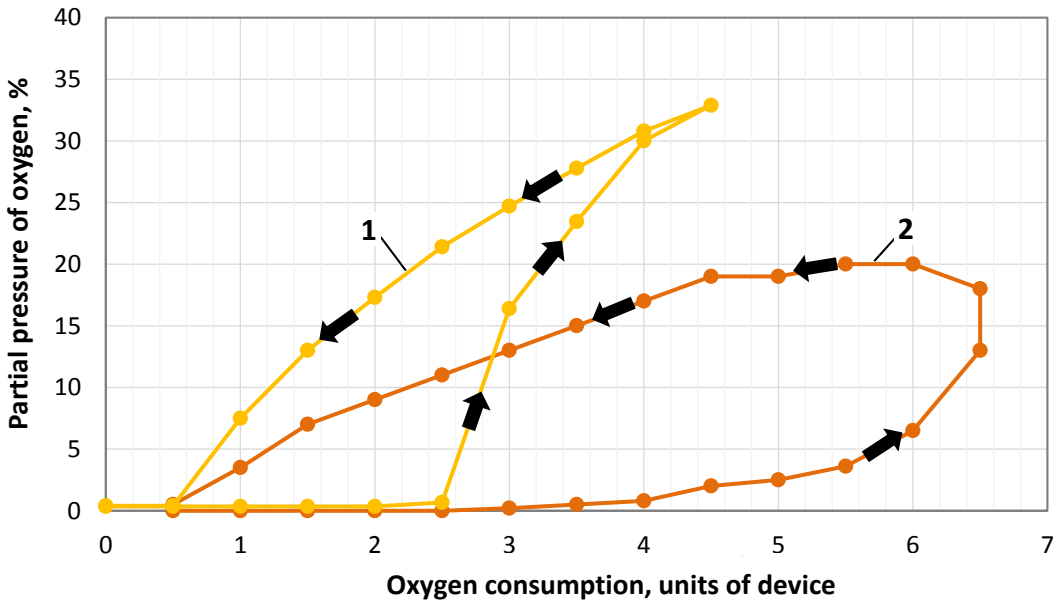

Fig. 4. *Dependence of the partial pressure of oxygen for cooled (1) and uncooled (2) targets on the oxygen consumption at a magnetron discharge power of 3 kW (the arrows show the direction of change in oxygen consumption)*
Рис. 4. *Зависимость парциального давления кислорода для охлаждаемой (1) и неохлаждаемой (2) мишеней от расхода кислорода при мощности магнетронного разряда 3 кВт (стрелками показано направление изменения расхода кислорода)*

Fig. 5 shows the measured dependence of the temperature of the uncooled and cooled targets on the magnetron discharge power. The cooled target temperature is determined by the thermal conductivity of the structure of target attachment to the magnetron magnetic system, so a linear dependence of the target temperature on the magnetron discharge power is obtained. The uncooled target temperature is determined by radiation from its surface, so a power dependence with a tendency to saturation is obtained.

From the comparison of the dependences of the partial pressure of argon and oxygen on the oxygen consumption for magnetron discharge powers of 3, 6 and 9 kW on an uncooled target, it is evident that an increase in the discharge power to 9 kW leads to a qualitative change in the type of hysteresis – the curve width decreases by more than 2 times (Fig. 6).

It was revealed that at a magnetron discharge power of more than 6 kW (the uncooled target temperature is more

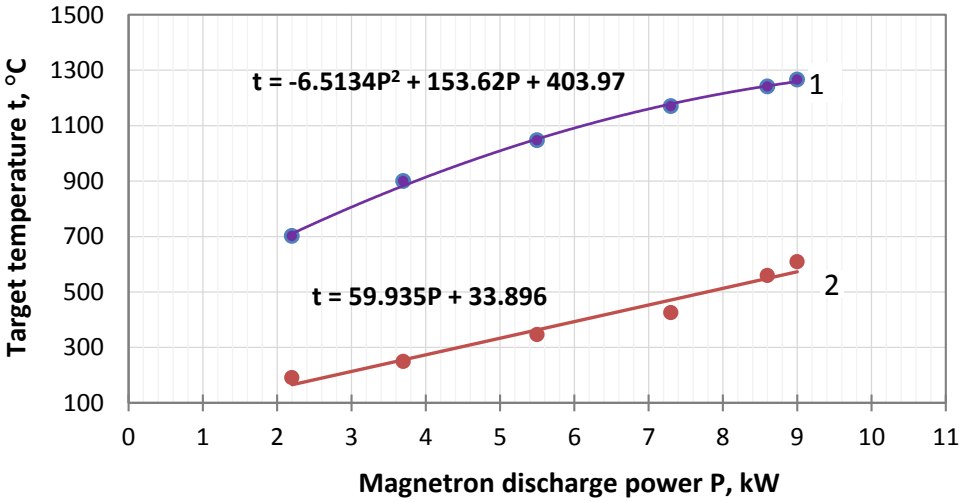

Fig. 5. *Dependence of temperatures of uncooled (1) and cooled (2) zirconium targets on the magnetron discharge power*
Рис. 5. *Зависимость температур неохлаждаемой (1) и охлаждаемой (2) циркониевых мишеней от мощности магнетронного разряда*

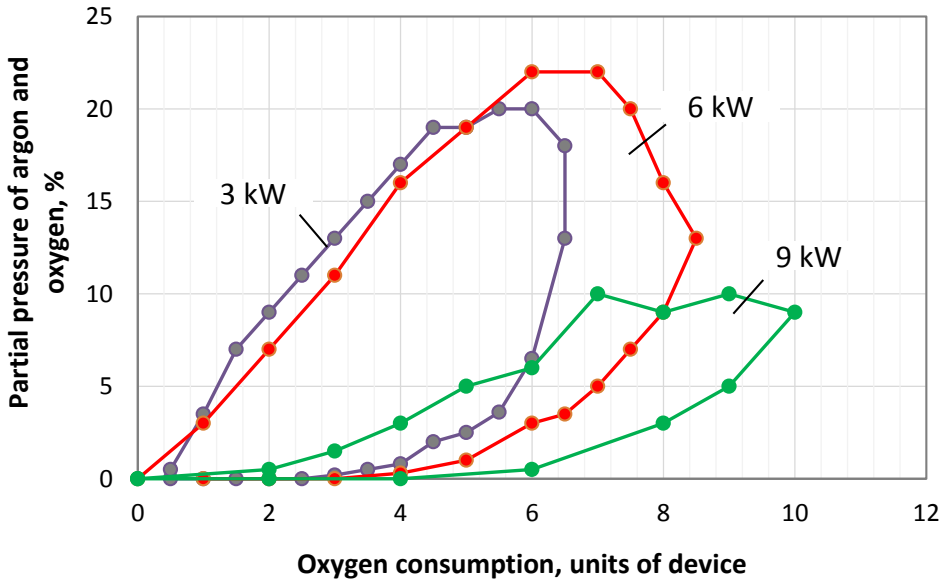

Fig. 6. *Dependence of the partial pressure of oxygen on oxygen consumption for various magnetron discharge capacities*
Рис. 6. *Зависимость парциального давления кислорода от расхода кислорода для различных мощностей магнетронного разряда на неохлаждаемой мишени*

than 1100 °C, Fig. 5), the type of the hysteresis curve (Fig. 6) changes qualitatively, and at a power of 9 kW, a significant narrowing of the hysteresis curve occurs. On the reverse branch of the obtained dependence for a power of 9 kW (Fig. 6), an extended range of values from 7.0 to 9.0 units of oxygen consumption is observed, at which the partial pressure of oxygen is stable.

The maximum value of the partial pressure of oxygen on the straight branches of the obtained hysteresis curves, allows judging the intensity of the process of oxygen absorption by the growing oxide film. Thus, an increase in power from 3 to 6 kW increased the maximum value of the partial pressure of oxygen, despite the fact that at a power of 6 kW the sputtering rate is at least 2 times greater than at 3 kW. An increase in power to 9 kW decreased the partial pressure of oxygen more than 2 times, which indicates a significant increase in the flow of sputtered atoms binding oxygen. This is also evidenced by the obtained data on measuring the deposition rate of the YSZ coating (Table 1).

Comparing the rates of deposition using cooled and uncooled targets (Table 1), showed that sputtering from an uncooled target allows increasing the deposition rate by more than 10 times, which is in qualitative agreement with the results of the study of the oxygen partial pressure (Fig. 4).

Fig. 7 shows the initial growth of a similar structure. The initial growth of the YSZ TBC feather structure obtained at a power of 8.7–8.8 kW is characterised by the growth of separately standing feathers with a dendritic structure having a width of 1 to 6 μm with gaps between them of 0.1–0.5 μm.

A study of the microstructure of the YSZ coating formed using an uncooled target at a power of 9 kW with a longer formation time compared to the coating shown in Fig. 7, showed a combination of nanolayer (with layer thicknesses from 60 to 140 nm) and columnar structures (Fig. 8).

When depositing on a polished surface (with *Ra* equal to 0.04÷0.06 μm) (Fig. 8 a), the width of the columns in the lower part of the coating is 0.2÷0.4 μm, in the upper part it varies from 0.4 to 2 μm (on average 0.9 μm), in the central layer of the coating, the columnar structure has a clearly visible dendritic structure. When forming a coating on a rougher surface (with *Ra* over 0.8 μm) (Fig. 8 b), a greater number of cracks and pores are observed, the width of the columns in the upper part of the coating increases reaching 2÷7 μm, the dendritic structure acquires a more pronounced feathery structure.

The study of the surface morphology by scanning electron microscopy showed that the surface of the YSZ coating with the corresponding microstructure shown in Fig. 8 b formed using an uncooled target has a hierarchical structure of the cauliflower type (Fig. 8 c). This structure at the nanolevel consists of grains with a diameter of 60÷90 nm, which are combined into blocks of 400÷600 nm, forming globules of 2÷4 μm at the microlevel, which, in turn, are combined into conglomerates up to 15 μm in size. The revealed structure of the formed coating of the cauliflower type at the micro level has porosity, which reduces the thermal conductivity coefficient.

Elemental EDS analysis of thermal barrier YSZ coatings formed using an uncooled target, showed the presence of 62÷67 wt. % of Zr, 8÷11 wt. % of Y, and 22÷30 wt. % of O.

Table 1. *Deposition rate of thermal barrier YSZ-coatings produced using cooled and uncooled targets*
Таблица 1. *Скорость осаждения термобарьерных YSZ-покрытий, полученных с использованием охлаждаемой и неохлаждаемой мишеней*

Magnetron type, power of 9 kW	Deposition rate, μm/h
With cooled target	0.7±0.2
With uncooled target	7.9±0.4

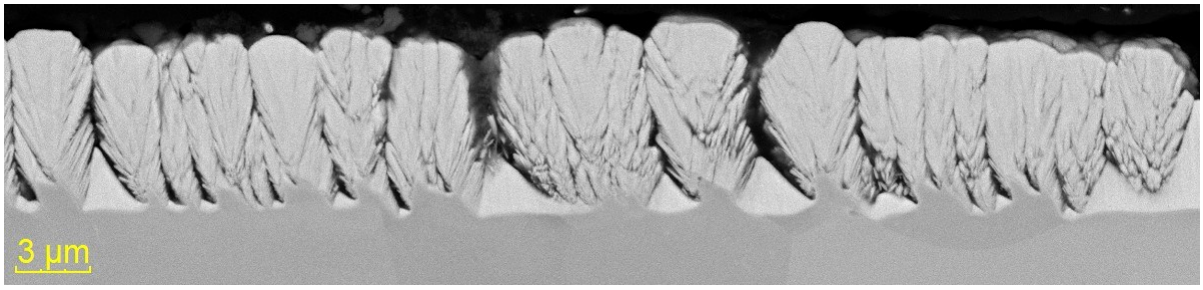

Fig. 7. *The structure of the thermal barrier YSZ-coating produced at a power of 8.7 kW*
Рис. 7. *Структура термобарьерного YSZ-покрытия, полученная при мощности 8,7 кВт*

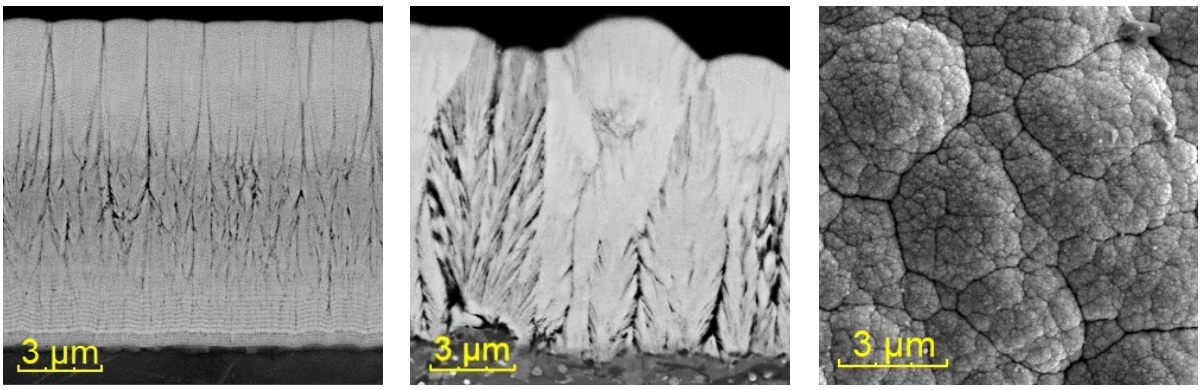

a *b* *c*

Fig. 8. *Transverse section (**a**, **b**) and surface morphology (**c**) of the thermal barrier YSZ-coating formed using an uncooled target at a power of 9 kW*
Рис. 8. *Поперечный шлиф (**a**, **b**) и морфология поверхности (**c**) термобарьерного YSZ-покрытия, сформированного с использованием неохлаждаемой мишени при мощности 9 кВт*

DISCUSSION

The known dependences of the partial pressure of oxygen on its consumption in the form of hysteresis loops, characteristic of the processes of formation of oxide films [15; 16], are also observed during their formation using an uncooled target. In this work, ranges of oxygen consumption values at various magnetron discharge powers are obtained, at which the work can be carried out with steady and stable process control. It was experimentally found that an increase in the temperature of the magnetron sputtering system target allows reducing the width of the hysteresis loop by 2 times.

Comparison of the deposition rates of the ZrYO-based coating on the oxygen consumption obtained for a cooled target (Fig. 1), and the deposition rates of the same coating obtained by the authors for an uncooled target, allows stating the fact of overcoming the occurrence of an oxide film and achieving a multiple increase in coating growth.

The data obtained in [16] that atoms are added to the main flow of sputtered atoms of the target material due to the sublimation process explain the observed fact of an increase in the oxide coating growth rate. One can assume with a high degree of probability that the sublimation process occurs from the entire heated surface of the target. However, at the same time, it should be expected that due to sublimation, the mechanical properties of the coating would change due to the difference in the energies of the sputtered and sublimated atoms, as was demonstrated in [17–19].

Thermal electron emission can occur from the heated surface of the oxide, which will increase the magnetron discharge current, and due to the heating of the uncooled target, oxide evaporation can occur in addition to sputtering. Consequently, on the uncooled target surface, an unambiguous relationship will be observed between three parameters determined by the target surface temperature: the growth rate of the oxide, the rate of its sputtering, and its conductivity.

Compared with the results for a cooled target shown in [8], the formation of coatings using an uncooled target also allows depositing films with high adhesion to the substrate, but requires a lower consumption of target material with a high coefficient of its use. In turn, a high adhesion value will limit the processes of destruction of coatings from [12; 14] at temperatures above 1300 °C.

The use of an uncooled target expands the possibilities of using target materials, and applying coatings to parts of complex shape, compared with the methods of electron beam evaporation, and plasma deposition in air [10; 11].

The YSZ coating formed using an uncooled target showed a combination of a nanolayer and columnar structure inherent in the structure of the thermal barrier coating produced in [20].

The obtained results open up new possibilities for the development of the technology for magnetron sputtering of an extended uncooled target for producing TBCs based on zirconium dioxide, partially stabilised by yttrium oxide, with a thickness of more than 50 μm and the study of their thermal and mechanical properties.

CONCLUSIONS

The results of the conducted studies of the technology of formation of thermal barrier coatings, show the possibility of using magnetron systems of sputtering of an extended uncooled target for the formation of a ceramic layer of TBC, with a developed porous structure.

It has been experimentally found that an increase in the magnetron target temperature, allows reducing the effect of hysteresis (the hysteresis loop width decreases by 2 times), and increasing the TBC deposition rate by more than 10 times compared to a cooled target.

REFERENCES

1. Banerjee P., Roy A., Sen S., Ghosh A., Saha G., Seikh A.H., Alnaser I.A. Ghosh M. Service life assessment of yttria stabilized zirconia (YSZ) based thermal barrier coating through wear behavior. *Heliyon*, 2023, vol. 9, no. 5, article number e16107. DOI: 10.1016/j.heliyon.2023.e16107.
2. Singh M., Sahu P.K., Sampath S., Jonnalagadda K.N. Fracture toughness of freestanding plasma sprayed

yttria stabilized zirconia coatings via in situ tensile experiments. *Journal of the European Ceramic Society*, 2024, vol. 44, no. 4, pp. 2499–2511. DOI: 10.1016/j.jeurceramsoc.2023.10.074.
3. Liu Qiaomu, Huang Shunzhou, He Aijie. Composite ceramics thermal barrier coatings of yttria stabilized zirconia for aero-engines. *Journal of Materials Science & Technology*, 2019, vol. 35, no. 12, pp. 2814–2823. DOI: 10.1016/j.jmst.2019.08.003.
4. Raza M., Boulet P., Pierson J.-F., Snyders R., Konstantinidis S. Thermal stability of oxygen vacancy stabilized zirconia (OVSZ) thin films. *Surface and Coatings Technology*, 2021, vol. 409, article number 126880. DOI: 10.1016/j.surfcoat.2021.126880.
5. De Goes W.U., Markocsan N., Gupta M., Vaßen R., Matsushita T., Illkova K. Thermal barrier coatings with novel architectures for diesel engine applications. *Surface and Coatings Technology*, 2020, vol. 396, article number 125950. DOI: 10.1016/j.surfcoat.2020.125950.
6. Yetim A.F., Tekdir H., Turalioglu K., Taftali M., Yetim T. Tribological behavior of plasma-sprayed Yttria-stabilized zirconia thermal barrier coatings on 316L stainless steel under high-temperature conditions. *Materials Letters*, 2023, vol. 336, article number 133873. DOI: 10.1016/j.matlet.2023.133873.
7. Karaoglan A.C., Ozgurluk Y., Gulec A., Ozkan D., Binal G. Effect of coating degradation on the hot corrosion behavior of yttria-stabilized zirconia (YSZ) and blast furnace slag (BFS) coatings. *Surface and Coatings Technology*, 2023, vol. 473, article number 130000. DOI: 10.1016/j.surfcoat.2023.130000.
8. Chen Can, Song Xuemei, Li Wei, Zheng Wei, Ji Heng, Zeng Yi, Shi Ying. Relationship between microstructure and bonding strength of yttria-stabilized zirconia thermal barrier coatings. *Ceramics International*, 2022, vol. 48, no. 4, pp. 5626–5635. DOI: 10.1016/j.ceramint.2021.11.107.
9. Sanjai S.G., Srideep S., Krishna B.A., Sumanth M.S., Ramaswamy P. Synthesis of Yttria-Stabilized Zirconia Nano Powders for Plasma Sprayed Nano Coatings. *Materials Today: Proceedings*, 2020, vol. 22, part 4, pp. 1253–1263. DOI: 10.1016/j.matpr.2020.01.418.
10. Wang Xin, Zhen Zhen, Huang Guanghong, Mu Rende, He Limin, Xu Zhenhua. Thermal cycling of EB-PVD TBCs based on YSZ ceramic coat and diffusion aluminide bond coat. *Journal of Alloys and Compounds*, 2021, vol. 873, article number 159720. DOI: 10.1016/j.jallcom.2021.159720.
11. Mulone A., Mahade S., Björklund S., Lundström D., Kjellman B., Joshi S., Klement U. Development of yttria-stabilized zirconia and graphene coatings obtained by suspension plasma spraying: Thermal stability and influence on mechanical properties. *Ceramics International*, 2023, vol. 49, no. 6, pp. 9000–9009. DOI: 10.1016/j.ceramint.2022.11.055.
12. Berlin E.V., Seydman L.A. *Poluchenie tonkikh plenok reaktivnym magnetronnym raspyleniem* [Production of thin films by reactive magnetron sputtering]. 2nd ed., ispr. i dop. Moscow, URSS Publ., 2022. 316 p.
13. Tkhabisimov A.B., Mednikov A.F., Dasaev M.R., Kachalin G.V., Zilova O.S. Solid particle erosion resistance of protective ion-plasma coating formed on full-scale objects based on modern additive technologies. *International Journal of Innovative Technology and Exploring Engineering*, 2019, vol. 8, no. 7, pp. 2295–2302. EDN: YNNMPC.
14. Dukhopelnikov D.V., Bulychev V.S., Vorobev E.V. Magnetron discharge with liquid-phase cathode. *Herald of the Bauman Moscow State Technical University, Series Natural Sciences*, 2018, no. 1, pp. 95–103. DOI: 10.18698/1812-3368-2018-1-95-103.
15. Kuritsyna I.E., Bredikhin S.I., Agarkov D.A., Borik M.A., Kulebyakin A.V., Milovich F.O., Lomonova E.E., Myzina V.A., Tabachkova N.Yu. Electrotransport characteristics of ceramic and single crystal materials with the $(ZrO_2)_{0.89}(Sc_2O_3)_{0.10}(Y_2O_3)_{0.01}$ composition. *Russian Journal of Electrochemistry*, 2018, vol. 54, pp. 481–485. DOI: 10.1134/S1023193518060125.
16. Zhang Wanying, Shi Fengyue, Wang Jianwen, Yang Yang, Zhao Guangdong, Zhao Dongyu. Preparation and properties of a porous ZrO_2/SiZrBOC ceramic matrix composite with high temperature resistance and low thermal conductivity. *Journal of the European Ceramic Society*, 2024, vol. 44, no. 4, pp. 2329–2337. DOI: 10.1016/j.jeurceramsoc.2023.11.007.
17. Lin Jianliang, Stinnett T.C. Development of thermal barrier coatings using reactive pulsed dc magnetron sputtering for thermal protection of titanium alloys. *Surface & Coatings Technology*, 2020, vol. 403, article number 126377. DOI: 10.1016/j.surfcoat.2020.126377.
18. Reddy G.V., Rasu N.G., Kumar M.M., Prasad J., Hari T. Review on Advanced Alternative Thermal Barrier Coatings (TBC's) Materials in Low Heat Rejection Engines. *International Journal of Research in Mechanical Engineering and Technology*, 2016, vol. 6, no. 2, pp. 27–35.
19. Bleykher G.A., Borduleva A.O., Krivobokov V.P., Sidelev D.V. Evaporation factor in productivity increase of hot target magnetron sputtering systems. *Vacuum*, 2016, vol. 132, pp. 62–69. DOI: 10.1016/j.vacuum.2016.07.030.
20. Chen Dianying, Dambra C., Dorfman M. Process and properties of dense and porous vertically-cracked yttria stabilized zirconia thermal barrier coatings. *Surface and Coatings Technology*, 2020, vol. 404, article number 126467. DOI: 10.1016/j.surfcoat.2020.126467.

СПИСОК ЛИТЕРАТУРЫ

1. Banerjee P., Roy A., Sen S., Ghosh A., Saha G., Seikh A.H., Alnaser I.A. Ghosh M. Service life assessment of yttria stabilized zirconia (YSZ) based thermal barrier coating through wear behavior // Heliyon. 2023. Vol. 9. № 5. Article number e16107. DOI: 10.1016/j.heliyon.2023.e16107.
2. Singh M., Sahu P.K., Sampath S., Jonnalagadda K.N. Fracture toughness of freestanding plasma sprayed yttria stabilized zirconia coatings via in situ tensile experiments // Journal of the European Ceramic Society. 2024. Vol. 44. № 4. P. 2499–2511. DOI: 10.1016/j.jeurceramsoc.2023.10.074.
3. Liu Qiaomu, Huang Shunzhou, He Aijie. Composite ceramics thermal barrier coatings of yttria stabilized zirconia for aero-engines // Journal of Materials Science & Technology. 2019. Vol. 35. № 12. P. 2814–2823. DOI: 10.1016/j.jmst.2019.08.003.

4. Raza M., Boulet P., Pierson J.-F., Snyders R., Konstantinidis S. Thermal stability of oxygen vacancy stabilized zirconia (OVSZ) thin films // Surface and Coatings Technology. 2021. Vol. 409. Article number 126880. DOI: 10.1016/j.surfcoat.2021.126880.
5. De Goes W.U., Markocsan N., Gupta M., Vaßen R., Matsushita T., Illkova K. Thermal barrier coatings with novel architectures for diesel engine applications // Surface and Coatings Technology. 2020. Vol. 396. Article number 125950. DOI: 10.1016/j.surfcoat.2020.125950.
6. Yetim A.F., Tekdir H., Turalioglu K., Taftali M., Yetim T. Tribological behavior of plasma-sprayed Yttria-stabilized zirconia thermal barrier coatings on 316L stainless steel under high-temperature conditions // Materials Letters. 2023. Vol. 336. Article number 133873. DOI: 10.1016/j.matlet.2023.133873.
7. Karaoglan A.C., Ozgurluk Y., Gulec A., Ozkan D., Binal G. Effect of coating degradation on the hot corrosion behavior of yttria-stabilized zirconia (YSZ) and blast furnace slag (BFS) coatings // Surface and Coatings Technology. 2023. Vol. 473. Article number 130000. DOI: 10.1016/j.surfcoat.2023.130000.
8. Chen Can, Song Xuemei, Li Wei, Zheng Wei, Ji Heng, Zeng Yi, Shi Ying. Relationship between microstructure and bonding strength of yttria-stabilized zirconia thermal barrier coatings // Ceramics International. 2022. Vol. 48. № 4. P. 5626–5635. DOI: 10.1016/j.ceramint.2021.11.107.
9. Sanjai S.G., Srideep S., Krishna B.A., Sumanth M.S., Ramaswamy P. Synthesis of Yttria-Stabilized Zirconia Nano Powders for Plasma Sprayed Nano Coatings // Materials Today: Proceedings. 2020. Vol. 22. Part 4. P. 1253–1263. DOI: 10.1016/j.matpr.2020.01.418.
10. Wang Xin, Zhen Zhen, Huang Guanghong, Mu Rende, He Limin, Xu Zhenhua. Thermal cycling of EB-PVD TBCs based on YSZ ceramic coat and diffusion aluminide bond coat // Journal of Alloys and Compounds. 2021. Vol. 873. Article number 159720. DOI: 10.1016/j.jallcom.2021.159720.
11. Mulone A., Mahade S., Björklund S., Lundström D., Kjellman B., Joshi S., Klement U. Development of yttria-stabilized zirconia and graphene coatings obtained by suspension plasma spraying: Thermal stability and influence on mechanical properties // Ceramics International. 2023. Vol. 49. № 6. P. 9000–9009. DOI: 10.1016/j.ceramint.2022.11.055.
12. Берлин Е.В., Сейдман Л.А. Получение тонких пленок реактивным магнетронным распылением. 2-е изд., испр. и доп. М.: URSS, 2022. 316 с.
13. Tkhabisimov A.B., Mednikov A.F., Dasaev M.R., Kachalin G.V., Zilova O.S. Solid particle erosion resistance of protective ion-plasma coating formed on full-scale objects based on modern additive technologies // International Journal of Innovative Technology and Exploring Engineering. 2019. Vol. 8. № 7. P. 2295–2302. EDN: YNNMPC.
14. Духопельников Д.В., Булычёв В.С., Воробьев Е.В. Магнетронный разряд с жидкофазным катодом // Вестник Московского государственного технического университета им. Н.Э. Баумана. Серия Естественные науки. 2018. № 1. С. 95–103. DOI: 10.18698/1812-3368-2018-1-95-103.
15. Kuritsyna I.E., Bredikhin S.I., Agarkov D.A., Borik M.A., Kulebyakin A.V., Milovich F.O., Lomonova E.E., Myzina V.A., Tabachkova N.Yu. Electrotransport characteristics of ceramic and single crystal materials with the $(ZrO_2)_{0.89}(Sc_2O_3)_{0.10}(Y_2O_3)_{0.01}$ composition // Russian Journal of Electrochemistry. 2018. Vol. 54. P. 481–485. DOI: 10.1134/S1023193518060125.
16. Zhang Wanying, Shi Fengyue, Wang Jianwen, Yang Yang, Zhao Guangdong, Zhao Dongyu. Preparation and properties of a porous ZrO_2/SiZrBOC ceramic matrix composite with high temperature resistance and low thermal conductivity // Journal of the European Ceramic Society. 2024. Vol. 44. № 4. P. 2329–2337. DOI: 10.1016/j.jeurceramsoc.2023.11.007.
17. Lin Jianliang, Stinnett T.C. Development of thermal barrier coatings using reactive pulsed dc magnetron sputtering for thermal protection of titanium alloys // Surface & Coatings Technology. 2020. Vol. 403. Article number 126377. DOI: 10.1016/j.surfcoat.2020.126377.
18. Reddy G.V., Rasu N.G., Kumar M.M., Prasad J., Hari T. Review on Advanced Alternative Thermal Barrier Coatings (TBC's) Materials in Low Heat Rejection Engines // International Journal of Research in Mechanical Engineering and Technology. 2016. Vol. 6. № 2. P. 27–35.
19. Bleykher G.A., Borduleva A.O., Krivobokov V.P., Sidelev D.V. Evaporation factor in productivity increase of hot target magnetron sputtering systems // Vacuum. 2016. Vol. 132. P. 62–69. DOI: 10.1016/j.vacuum.2016.07.030.
20. Chen Dianying, Dambra C., Dorfman M. Process and properties of dense and porous vertically-cracked yttria stabilized zirconia thermal barrier coatings // Surface and Coatings Technology. 2020. Vol. 404. Article number 126467. DOI: 10.1016/j.surfcoat.2020.126467.

К вопросу о формировании термобарьерных покрытий методом магнетронного распыления

Качалин Геннадий Викторович[1], кандидат технических наук, ведущий научный сотрудник
Медведев Константин Сергеевич[2], ведущий инженер
Медников Алексей Феликсович[3], кандидат технических наук, ведущий научный сотрудник
Зилова Ольга Сергеевна[4], кандидат технических наук, ведущий научный сотрудник
Тхабисимов Александр Борисович*[5], кандидат технических наук, старший научный сотрудник
Илюхин Дмитрий Игоревич[6], инженер 1 категории
Касьяненко Владислав Александрович[7], инженер 1 категории
Национальный исследовательский университет «МЭИ», Москва (Россия)

*E-mail: TkhabisimovAB@mpei.ru,
abt-bkt@mail.ru

[1]ORCID: https://orcid.org/0000-0001-9506-862X
[2]ORCID: https://orcid.org/0000-0003-1667-458X
[3]ORCID: https://orcid.org/0000-0003-4883-7873
[4]ORCID: https://orcid.org/0000-0002-0410-8188
[5]ORCID: https://orcid.org/0000-0001-9544-9086
[6]ORCID: https://orcid.org/0009-0009-6385-0284
[7]ORCID: https://orcid.org/0009-0000-7510-2106

Received 18.10.2024 *Revised 26.11.2024* *Accepted 03.12.2024*

Аннотация: Применение магнетронных распылительных систем с протяженными неохлаждаемыми мишенями позволит разработать промышленные импортозамещающие технологии формирования термобарьерных покрытий на основе оксида циркония, легированного оксидами редкоземельных металлов, для решения актуальных задач газового турбостроения. В работе приведены результаты сравнения технологии получения термобарьерных покрытий методом магнетронного распыления с двумя типами протяженных мишеней из сплава Zr–8%Y – широко распространенной и применяемой охлаждаемой мишенью и разрабатываемой авторами неохлаждаемой протяженной мишенью магнетронной распылительной системы. Приведено сравнение результатов масс-спектрометрических исследований гистерезиса парциального давления кислорода, свойственного технологии получения оксидных пленок; влияния типа мишени на скорость роста покрытия; исследований методом растровой электронной микроскопии структуры термобарьерных покрытий; элементного состава покрытий на основе диоксида циркония, частично стабилизированного оксидом иттрия – YSZ. Экспериментально установлено, что повышение температуры мишени магнетронной распылительной системы позволяет в 2 раза уменьшить ширину петли характерного гистерезиса зависимости парциального давления кислорода от его расхода. Полученные зависимости позволили определить диапазон значений расхода кислорода при различных мощностях магнетронного разряда, при которых работа может производиться с устойчивым и стабильным управлением процесса, без опасности попадания в гистерезис. Проведенные металлографические исследования показали характерную развитую пористую дендритную структуру керамического слоя, необходимую для снижения коэффициента теплопроводности термобарьерного покрытия. Выявлено, что применение неохлаждаемой мишени позволяет повысить скорость осаждения термобарьерного покрытия более чем в 10 раз по сравнению со скоростью осаждения для охлаждаемой мишени. Полученные результаты демонстрируют возможность применения технологии магнетронного распыления протяженной неохлаждаемой мишени для формирования керамического слоя термобарьерных покрытий.

Ключевые слова: магнетронное распыление; неохлаждаемая мишень; термобарьерные покрытия; гистерезисные явления; скорость осаждения покрытия.

Благодарности: Государственное задание № FSWF-2023-0016 (соглашение № 075-03-2023-383 от 18 января 2023 г.) в сфере научной деятельности на 2023–2025 гг.

Для цитирования: Качалин Г.В., Медведев К.С., Медников А.Ф., Зилова О.С., Тхабисимов А.Б., Илюхин Д.И., Касьяненко В.А. К вопросу о формировании термобарьерных покрытий методом магнетронного распыления // Frontier Materials & Technologies. 2024. № 4. С. 51–61. DOI: 10.18323/2782-4039-2024-4-70-5.